Metal Nanoparticles as An Alternative to Antimycotics

Subjects: Microbiology

Contributor: Yael N. Slavin , Horacio Bach

Fungi were initially included as a part of Kingdom Plantae but in 1969 were grouped into Kingdom Fungi, which comprises diverse groups with different morphologies, such as unicellular yeasts and multicellular organisms. The rate of antifungal resistance development has been called “unprecedented”. This is because immunocompromised individuals are at a higher risk of fungal infections than healthy individuals. Moreover, medical advancements over the past few decades and the HIV epidemic have increased the number of immunocompromised people, which has, in turn, shifted fungal infections from being an infrequent cause of disease to being an important contributor to human morbidity and mortality worldwide. There are six antifungal drug classes, and this scarcity, combined with the increasing resistance, has led to the need for novel treatments. The appearance of resistant species of fungi to the existent antimycotics is challenging for the scientific community. One emergent technology is the application of nanotechnology to develop novel antifungal agents. Metal nanoparticles (NPs) have shown promising results as an alternative to classical antimycotics.

nanoparticles metals ROS

1. Nanoparticle Formulation as Antifungal Agents

There is a need for novel antifungal treatments as currently available options are lacking. It is worth noting that the idea of increased potential future resistance is worrying as fungi are eukaryotes, as are their most common hosts found in Kingdoms Animalia and Plantae. That is to say, the eukaryotic hosts of pathogenic fungi have similarities in metabolism and protein structure, and finding targets to differentiate organisms becomes more complicated [1].

Nanotechnology has rapidly progressed over the past few decades and using nanoparticles (NPs) as potential antifungals have been an expanding field of interest. The present study summarized the literature from 2005 until 2022 regarding the NP formulations that showed antifungal activity (**Table 1**, **Table 2**, **Table 3**, **Table 4**, **Table 5** and **Table 6**). A summary of the different types of metallic NPs studied is shown in **Figure 1**.

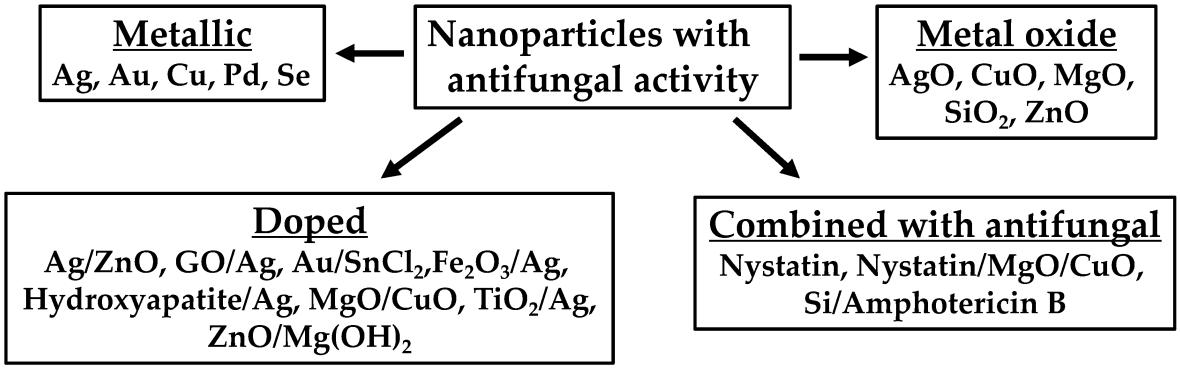

Figure 1. Different types of metallic NPs developed against fungi.

Table 1. Activities of NPs tested on different fungal species expressed in MIC_{100} (µg/mL).

Type of NP	Shape	Size (nm)	Organism(s) Tested	MIC_{100} (µg/mL)	Reference
Ag	Spherical	3	*Saccharomyces cerevisiae* (KCTC 7296) *Trichosporon beigelii* (KCTC 7707) *Candida albicans* (ATCC 90028)	2	[2]
	Spherical	1–21	*Candida albicans* *Candida glabrata* *Candida parapsilosis* *Candida tropicalis* *Fusarium solani* *Fusarium moniliforme* *Fusarium oxysporum* *Aspergillus flavus* *Aspergillus fumigatus* *Aspergillus terrus* *Sporothrix schenckii* *Cryptococcus neoformans*	0.25 0.125 0.25 0.125 1 2 4 1 2 2 0.25 0.25	[3]
	Spherical	5	*Candida albicans* (324LA/84) *Candida glabrata* (ATCC 90030) *Candida albicans* (ATCC 10321) *Candida glabrata* (D1)	0.4–0.8 0.4–0.8 0.8–1.6 1.6–3.3	[4]
	Spherical	7	*Aspergillus flavus* *Aspergillus fumigatus*	100 100	[5]

Type of NP	Shape	Size (nm)	Organism(s) Tested	MIC_{100} (μg/mL)	Reference
	Spherical	25	*Candida albicans* (I) *Candida albicans* (II) *Candida parapsilosis* *Candida tropicalis*	0.42 0.21 1.690 0.840	[6]
	Spherical	5–20	*Trichosporon asahii* (CBS2479) *Trichosporon asahii* (BZ701) *Trichosporon asahii* (BZ702) *Trichosporon asahii* (BZ703) *Trichosporon asahii* (BZ704) *Trichosporon asahii* (BZ705) *Trichosporon asahii* (BZ705R) *Trichosporon asahii* (BZ901) *Trichosporon asahii* (BZ902) *Trichosporon asahii* (BZ121) *Trichosporon asahii* (BZ122) *Trichosporon asahii* (BZ123) *Trichosporon asahii* (BZ124) *Trichosporon asahii* (BZ125) *Trichosporon asahii* (CBS8904) *Trichosporon asahii* (CBS7137) *Trichosporon asahii* (CBS8520)	0.50 0.67 0.50 1.00 0.67 0.50 0.50 0.67 1.00 0.83 0.67 0.50 0.67 0.83 0.50 0.67 0.67	[7]
	Spherical	15–25	*Candida albicans* (ATCC 10231) *Candida albicans* (ATCC 90028) *Candida glabrata* (ATCC 90030) *Candida parapsilosis* (ATCC 22019)	1.56 6.25 3.12 6.25	[8]

Type of NP	Shape	Size (nm)	Organism(s) Tested	MIC_{100} (μg/mL)	Reference
	Spherical	25	*Candida albicans* (I) *Candida albicans* (II) *Candida parapsilosis* *Candida tropicalis*	27 27 27 27	[6]
	Spherical to polyhedric	73.72	*Trichophyton rubrum* (*n* = 8) *Trichophyton rubrum* (ATCC MYA 4438)	0.5–2.5 <0.25	[9]
	Spherical	76.14	*Trichophyton rubrum* (*n* = 8) *Trichophyton rubrum* (ATCC MYA 4438)	>7.5 >7.5	[9]
	Spherical	100.6	*Trichophyton rubrum* (*n* = 8) *Trichophyton rubrum* (ATCC MYA 4438)	0.5–5 0.5	[9]
	NR	NR	*Fusarium graminearum*	4.68	[10]
	NR	NR	*Candida albicans* (I) *Candida albicans* (II) *Candida parapsilosis* *Candida tropicalis*	0.42 0.21 1.69 0.84	[6]
	NR	NR	*Candida albicans* (I) *Candida albicans* (II) *Candida parapsilosis* *Candida tropicalis*	0.052 0.1 0.84 0.42	[6]
	NR	NR	*Candida albicans* (I) *Candida albicans* (II) *Candida parapsilosis* *Candida tropicalis*	3.38 3.38 3.38 3.38	[6]
	NR	20–25	*Aspergillus niger* *Candida albicans* *Cryptococcus neoformans*	25 6 3	[11]
	NR	NR	*Fusarium graminearum*	12.5	[10]
Ag/ZnO	Spherical	7/477	*Aspergillus flavus* *Aspergillus fumigatus*	50/10 50/10	[5]
qAg	Spherical	2–3	*Candida albicans*	0.07	[12]

Type of NP	Shape	Size (nm)	Organism(s) Tested	MIC_{100} (μg/mL)	Reference
Cu	Spherical	10–40	*Candida albicans* (ATCC 10231) *Candida albicans* (Clinical strain C) *Candida albicans* (Clinical strain E)	129.7 1037.5 518.8	[13]
	Wires	20–30 μm, 30–60 nm diameter	*Candida albicans* (ATCC 10231) *Candida albicans* (Clinical strain C) *Candida albicans* (Clinical strain E)	260.3 260.3 260.3	[13]
γ-Fe_2O_3/Ag	NR	20–40 (Ag) + 5 (γ-Fe_2O_3)	*Candida albicans* (I) *Candida albicans* (II) *Candida tropicalis* (5) *Candida parapsilosis* (6)	1.9 1.9 31.3 31.3	[14]
Fe_3O_4/Ag	NR	~5 (Ag) + ~70 (Fe_3O_4)	*Candida albicans* (I) *Candida albicans* (II) *Candida tropicalis* (5) *Candida parapsilosis* (6)	1.9 1.9 3.9 7.8	[14]
GO/Ag	Spherical	10–35	*Fusarium graminearum*	9.37	[10]
HA/Ag	Rod/Spherical	12–27	*Candida albicans*	62.5	[15]
MgO 500 °C calcination	Flaked layers	52 ± 18	*Colletotrichum gloeosporioides* (from papaya) *Colletotrichum gloeosporioides* (from avocado)	156 312	[16]
MgO 1000 °C calcination	Flaked layers	96 ± 33	*Colletotrichum gloeosporioides* (from papaya) *Colletotrichum gloeosporioides* (from avocado)	312 312	[16]
Pd	Spherical	9 ± 3.9	*Candida albicans* (ATCC 10231) *Aspergillus niger*	212.5 200	[17]
Se	Spherical	80–200	*Candida albicans* (ATCC 76615)	100 70	[18]

Type of NP	Shape	Size (nm)	Organism(s) Tested	MIC_{100} (μg/mL)	Reference
			Candida albicans (ATCC 10231)		
Se	Spherical	37–46	*Aspergillus fumigatus* (TIMML-025) *Aspergillus fumigatus* (TIMML-050) *Aspergillus fumigatus* (TIMML-379)	0.5 0.5 1	[19]
Silica/AmB	NR	5	*Candida albicans* *Candida krusei* *Candida parapsilosis* *Candida glabrata* *Candida tropicalis*	100 1000 1000–2000 300 100	[20]
TiO_2/Ag + $NaHB_4$	NR	250–300	*Aspergillus niger* *Candida albicans* *Cryptococcus neoformans*	25 12.5 12.5	[11]
TiO_2/Ag + UV	NR	250–300	*Aspergillus niger* *Candida albicans* *Cryptococcus neoformans*	12.5 6 3	[11]
ZnO	Spherical	20–40	*Candida albicans* (*n* = 125)	0.2–296	[21]
	Spherical	477	*Aspergillus flavus* *Aspergillus fumigatus*	20 20	[5]
ZnO 500 °C calcination	Spherical + cylindrical	51 ± 13	*Colletotrichum gloeosporioides* (from papaya) *Colletotrichum gloeosporioides* (from avocado)	156 312	[16]
ZnO 1000 °C calcination	Hexagonal bars	53 ± 17	*Colletotrichum gloeosporioides* (from papaya) *Colletotrichum gloeosporioides* (from avocado)	156 312	[16]
$ZnO/Mg(OH)_2$ 25 °C synthesis	Flakes + bars	54 ± 17	*Colletotrichum gloeosporioides* (from papaya)	156 312	[16]

Type of NP	Shape	Size (nm)	Organism(s) Tested	MIC_{100} (µg/mL)	Reference
			Colletotrichum gloeosporioides (from avocado)		
ZnO NP 25 °C synthesis	Hexagonal bars + ovoidal	63 ± 18	*Colletotrichum gloeosporioides* (from papaya) *Colletotrichum gloeosporioides* (from avocado)	312 312	[16]
$ZnO/Mg(OH)_2$ 70 °C synthesis	Flakes + bars	71 ± 22	*Colletotrichum gloeosporioides* (from papaya) *Colletotrichum gloeosporioides* (from avocado)	312 312	[16]
ZnO 25 °C synthesis, hydrothermal	Prisms with pyramidal ends	77 ± 31	*Colletotrichum gloeosporioides* (from papaya) *Colletotrichum gloeosporioides* (from	312 312	[16]

Type of NP	Shape	Size (nm)	Organism(s) Tested	MIC_{50} (µg/mL)	Reference
Ag	Spherical	30–50	*Candida albicans* (*n* = 30) *Candida glabrata* (*n* = 30) *Candida tropicalis* (*n* = 30)	4 9 9	[23]
Ag	Cubical	40–50	*Candida albicans* (*n* = 30) *Candida glabrata* (*n* = 30) *Candida tropicalis* (*n* = 30)	1 7 7	[23]
Ag	Wires	250–300	*Candida albicans* (*n* = 30) *Candida glabrata* (*n* = 30) *Candida tropicalis* (*n* = 30)	5 12 11	[23]
Au	Cubical	30–50	*Candida albicans* (*n* = 30) *Candida glabrata* (*n* = 30) *Candida tropicalis* (*n* = 30)	3 10 11	[23]
Au	Spherical	35–50	*Candida albicans* (*n* = 30) *Candida glabrata* (*n* = 30) *Candida tropicalis* (*n* = 30)	8 13 12	[23]
Au	Wires	300–500	*Candida albicans* (*n* = 30) *Candida glabrata* (*n* = 30) *Candida tropicalis* (*n* = 30)	7 15 15	[23]
ZnO	Spherical	20–40	*Candida albicans* (*n* = 125)	8.2	[21]
ZnO	NR	NR	*Candida albicans* (*n* = 10)	5	[22]

Table 3. Activities of NPs tested on different fungal species expressed as MIC_{80} (µg/mL).

Type of NP	Shape	Size (nm)	Organism(s) Tested	MIC_{80} (µg/mL)	Reference
AuNP + $SnCl_2$ as reducing agent	Polygonal, almost spherical	5–50	*Candida albicans* *Candida tropicalis* *Candida glabrata*	16 16 16	[24]
AuNP + $NaBH_4$ as reducing agent	Spherical	3–20	*Candida albicans* *Candida tropicalis* *Candida glabrata*	4 4 4	[24]
			avocado)	90	
			Candida albicans (*n* =	0.02–	[22]

Type of NP	Shape	Size (nm)	Organism(s) Tested	MIC_{90} (µg/mL)	Reference
LMW Chitosan NP ± 1 mg/mL chitosan	Spherical	174 ± 38.47	*Candida albicans* *Fusarium solani* *Aspergillus niger*	250 1000 NR	[25]
HMW Chitosan NP ± 1 mg/mL chitosan	Spherical	210 ± 24.54	*Candida albicans* *Fusarium solani* *Aspergillus niger*	1000 500 NR	[25]
LMW Chitosan NP ± 2 mg/mL chitosan	Spherical	233 ± 41.38	*Candida albicans* *Fusarium solani* *Aspergillus niger*	857.2 857.2 NR	[25]
HMW Chitosan NP ± 2 mg/mL chitosan	Spherical	263 ± 86.44	*Candida albicans* *Fusarium solani* *Aspergillus niger*	857.2 857.2 1714	[25]
LMW Chitosan NP ± 3 mg/mL chitosan	Spherical	255 ± 42.81	*Candida albicans* *Fusarium solani* *Aspergillus niger*	607.2 1214 NR	[25]
HMW Chitosan NP ± 3 mg/mL chitosan	Spherical	301 ± 72.85	*Candida albicans* *Fusarium solani* *Aspergillus niger*	607.2 1214.3 2428.6	[25]
Ag	Cubical	40–50	*Candida albicans* (*n* = 30) *Candida glabrata* (*n* = 30) *Candida tropicalis* (*n* = 30)	8 30 31	[23]
Ag	Spherical	30–50	*Candida albicans* (*n* = 30) *Candida glabrata* (*n* = 30) *Candida tropicalis* (*n* = 30)	11 37 35	[23]

Type of NP	Shape	Size (nm)	Organism(s) Tested	MIC_{90} (μg/mL)	Reference
Ag	Wires	250–300	*Candida albicans* (*n* = 30) *Candida glabrata* (*n* = 30) *Candida tropicalis* (*n* = 30)	21 51 48	[23]
Au	Cubical	30–50	*Candida albicans* (*n* = 30) *Candida glabrata* (*n* = 30) *Candida tropicalis* (*n* = 30)	10 45 46	[23]
Au	Spherical	35–50	*Candida albicans* (*n* = 30) *Candida glabrata* (*n* = 30) *Candida tropicalis* (*n* = 30)	15 47 48	[23]
Au	Wires	300–500	*Candida albicans* (*n* = 30) *Candida glabrata* (*n* = 30) *Candida tropicalis* (*n* = 30)	30 70 73	[23]
ZnO	Spherical	20–40	*Candida albicans* (*n* = 125)	17.76	[21]

n).

Type of NP	Shape	Size (nm)	Organism(s) Tested	Activity (mm)	Reference
CuO	Spherical	3–30	*Fusarium equiseti* *Fusarium oxysporum* *Fusarium culmorum*	25 20 19	[26]
Pd	Spherical	200	*Colletotrichum gloeosporioides*	Day 2: 3.6 Day 4: 1.6	[27]
			Fusarium oxysporum	Day 2: 12.2 Day 4: 10.9	
Pd	Spherical	220	*Colletotrichum gloeosporioides*	Day 2: 7.9 Day 4: 6.3	[27]
			Fusarium oxysporum	Day 2: 5.1 Day 4: 4.7	
Pd	Spherical	250	*Colletotrichum gloeosporioides*	Day 2: 2.4 Day 4: 0.7	[27]

ecular-

Type of NP	Shape	Size (nm)	Organism(s) Tested	Activity (mm)	Reference
			Fusarium oxysporum	Day 2: 10.4 Day 4: 9.6	
Pd	Spherical	350	*Fusarium oxysporum*	Day 2: 1.5 Day 4: 1.3	[27]
Pd	Spherical	550	*Fusarium oxysporum*	Day 2: 3.8 Day 4: 3.3	[27]
Nystatin/MgO/CuO	Spherical	8000–10000	*Candida albicans* (AH201) *Candida albicans* (AH267)	24.5 ± 1.7 14.3 ± 1.2	[28]
Nystatin	Spherical	8000–10000	*Candida albicans* (AH201) *Candida albicans* (AH267)	0.41 ± 0.23 0.5 ± 0.21	[28]
MgO/CuO	Spherical	8000–10000	*Candida albicans* (AH201) *Candida albicans* (AH267)	19.2 ± 1.6 1.3 ± 0.61	[28]
TiO_2/BPE B	NR	NR	*Candida albicans* (ATCC 14053)	11.2 ± 0.02	[29]
TiO_2/BPE C	NR	NR	*Candida albicans* (ATCC 14053)	15.9 ± 0.04	[29]
TiO_2/BPE D	NR	NR	*Candida albicans* (ATCC 14053)	13.5 ± 0.04	[29]
TiO_2/BPE E	NR	NR	*Candida albicans* (ATCC 14053)	14.6 ± 0.01	[29]
TiO_2/BPE B	NR	NR	*Penicillum chrysogenum* (MTCC 5108)	10.2 ± 0.05	[29]
TiO_2/BPE C	NR	NR	*Penicillum chrysogenum* (MTCC 5108)	18.0 ± 0.03	[29]
TiO_2/BPE D	NR	NR	*Penicillum chrysogenum* (MTCC 5108)	15.0 ± 0.04	[29]

Type of NP	Shape	Size (nm)	Organism(s) Tested	Activity (%)	Reference
Ag	NR	20–100	*Cladosporium cladosporioides* *Aspergillus niger*	50 µg/mL → 90 50 µg/mL → 70	[30]
Ag	Polygonal	35 ± 15	*Candida tropicalis* *Saccharomyces boulardii*	25 µg/mL → >95 50 µg/mL → >95 25 µg/mL → <50 50 µg/mL → >95	[31]
Ag	Spherical	5	*Colletotrichum gloeosporioides*	13 µg/mL → 73 26 µg/mL → 82 56 µg/mL → 89	[32]
Ag	Spherical	24	*Colletotrichum gloeosporioides*	13 µg/mL → 74 26 µg/mL → 82 56 µg/mL → 89	[32]

Type of NP	Shape	Size (nm)	Organism(s) Tested	Activity (%)	Reference
ZnO	Spherical	30–45	*Erythricium salmonicolor*	12 mmol/L, day 7 → 71.3 12 mmol/L, day 10 → 51.1 9 mmol/L, day 7 → 58.3 9 mmol/L, day 10 → 44.6 6 mmol/L, day 7 → 48.9 6 mmol/L, day 10 → 23.6 3 mmol/L, day 7 → 36.9 3 mmol/L, day 10 → 14.1	[33]
Ag	NR	NR	*Rhizoctonia solani* (AG1)	6 µg/mL → 75 8 µg/mL → 80 10 µg/mL → 90 12 µg/mL → 90 14 µg/mL → 90 16 µg/mL → 100	[34]
			Rhizoctonia solani (AG4)	6 µg/mL → ≥90 8 µg/mL → ≥90 10 µg/mL → ≥90 12 µg/mL → 100 14 µg/mL → 100 16 µg/mL → 100	
			Macrophomina phaseolina	6 µg/mL → 100 8 µg/mL → 100 10 µg/mL → 100 12 µg/mL → 100 14 µg/mL → 100 16 µg/mL → 100	
			Sclerotinia sclerotiorum	6 µg/mL → ≥95 8 µg/mL → 100 10 µg/mL → 100 12 µg/mL → 100 14 µg/mL → 100 16 µg/mL → 100	
			Trichoderma harzianum	6 µg/mL → 80 8 µg/mL → 84 10 µg/mL → 90 12 µg/mL → 100 14 µg/mL → 100 16 µg/mL → 100	
			Pythium aphanidermatum	6 µg/mL → 100 8 µg/mL → 100 10 µg/mL → 100 12 µg/mL → 100 14 µg/mL → 100 16 µg/mL → 100	
Ag	Spherical	10–20	*Bipolaris sorokiniana*	≥2 µg/mL → 100	[35]

Type of NP	Shape	Size (nm)	Organism(s) Tested	Activity (%)	Reference
Ag	Spherical	1–9	*Aspergillus flavus*	5 µg/mL → 0 15 µg/mL → 30 25 µg/mL → 58 35 µg/mL → 85 45 µg/mL → 98 60 µg/mL → 100	[36]
PEI[1]/Ag	Spherical	20.6	*Rhizopus arrhizus*	1.6 µg/mL → 97	[37]
PEI[2]/Ag	Spherical	4.24		6.5 µg/mL → 94	[27]
SiO_2	Spherical	9.92–19.8	*Rhizoctonia solani*	100 µg/mL → 93–100	[38]

small size
l particles
m smaller
ogeneous
e, altering
embly [10].
nicals and
usually, a
loride [24]
[39].

There is no standardized approach to the fabrication of NPs, and they have been found in various shapes, sizes, compositions, and formulations. However, spherical AgNPs are the most popular. Ag has been known for centuries to possess antimicrobial properties [40]. We know today that AgNPs possess these same properties and unique optical, electrical, and other physical/chemical properties. It is proposed that a potential mechanism of toxicity of Ag comes from its ion release coupled with its catalytic oxidation abilities [41].

Combining different AgNPs can exhibit a synergistic effect [42]. For example, combinations of AgNPs with other oxides, such as maghemite (γ-Fe_2O_3) or magnetite (Fe_3O_4), can lead to NPs that possess the unique Ag features while incorporating the magnetic features included in the iron oxide compounds, such as controllable alterations through magnetic field manipulation [14]. Moreover, combining AgNPs with graphene-oxide (GO) produced nanosheets with a three- and a seven-fold increase in bacterial inhibition efficiency over their counterparts in one study [10]. However, in another, combining AgNPs with ineffective copper NPs (CuNPs), a synergistic effect was not measured but somewhat diminished the activity of the AgNPs [43].

Other types of oxides have been investigated as well. A study looking at the antifungal activity of metal(loid) oxides found that Al_2O_3, Mn_3O_4, SiO_2, and SnO_2 reduced cell viability in a dose-dependent manner, whereas In_2O_3 showed no toxicity, even at concentrations of 100 mg/L [44]. GO is also of interest and has been used in functionalization and investigated as it is a single-atom-thick and a 2D sp^2-bonded carbon lattice with a large surface area [45]. This is important because a lattice will innately prevent aggregation as dispersion will be enhanced and remain during the usage of the particles. Thus, GO's surfactant-like properties allow it to attach metal NPs to hyphal interfaces, forming nanosheets with concomitant mechanical damage due to their extremely sharp edges [10].

Other oxides, such as titanium dioxide (TiO_2) NPs, have shown that the mechanism of antimicrobial ability requires visible light to affect [46][47]. The photocatalytic activity is based on hydroxyl radical generation. It is known that photocatalysis works through photons exciting electrons to the conduction band and forming electron-hole pairs. An alternative to increase the radical hydroxyl production is doping TiO_2 with Ag, potentially by accepting the

photoinduced electrons and holes with an increase in the degradation efficiency [47]. Another study found that undoped TiO_2NPs did have some antifungal properties, but the combination with Ag enhanced their efficacy. Fungal species also play a role in the antifungal activity of NPs, e.g., *Venturia inaequalis* was more affected by undoped TiO_2 than *Fusarium solani*. Still, the most effective nanomaterial was Ag-doped hollow TiO_2NPs. However, this may have been because the hollow formulation was spherical, and the solid formulation shape was indiscernible in TEM imaging [47]. As shown in another study, TiO_2NPs did not show activity unless doped with nitrogen (N) and fluorine (F) [46]. Lastly, zinc oxide (ZnO) NPs are a prevalent oxide formulation [48][49][50][51][52].

Green synthesis is a method of synthesizing NPs that is more biologically- and environmentally friendly. This is done by using biogenic sources such as plants, bacteria, or fungi and incorporating their naturally occurring innately-antimicrobial metabolites or compounds into or onto NPs, acting as stabilizers or removing the need for harsh chemical components [53][54]. Sometimes, the color of the NPs may change when using plant extracts to synthesize NPs. For instance, a change to red/brown may indicate the incorporation of saponins and phenolic compounds as stabilizing agents providing the reduction power during production [55]. In another study, encapsulated *Cymbopogon martinii* (ginger grass) essential oil (extracted through hydro distillation) rather than using plant extracts during formulation in chitosan NPs to exploit the oil's antifungal properties against *Fusarium graminearum* [53].

NPs made with biogenic sources [8][9][18][30][52][54][55][56][57] can have an enhanced effect compared to NPs made only chemically [52]. The biogenic formulation can increase the antifungal effect via increased reactive oxygen species (ROS) production, cell membrane disintegration, spore reduction, gene expression changes, and mycelial destruction [8][18][19][50][52]. Upon altering parameters, biogenic sources may produce AgNPs less effective than their chemical-only counterparts. An important parameter is a biological source; for example, the use of the fungus *Penicillium chrysogenum* as part of the synthesis of AgNPs was more effective than *A. oryzae*, although still less effective than the chemical-only process [9]. The formulation process may differ from organism to organism; however, the metal ions are typically entrapped by or surrounded by compounds released from the microorganism and undergo reduction.

Since fungal culture is a lab-controlled environment, the parameters for the formulation of NPs are also controlled [58]. For example, He et al. hypothesized that during gold NPs (AuNPs) formation, the bacterium *Rhodopseudomonas capsulate* secrets NADH- and NADH-dependent enzymes. During the electron transfer from NADH by NADH-dependent reductase, Au (III) ions capture electrons and, as a result, are reduced to Au (0) [59]. This mechanism of NADH- and NADH-dependent enzymes is likely also present in fungi, as extracellular filtrate of *F. oxysporum* strains used for synthesis contained NADH-dependent nitrate reductase enzymes [60].

Fungal biomolecules can behave as stabilizing agents during the formulation process and help achieve spherical particles [9][54]. For instance, during AuNPs formulation, it was found that biomolecules >3 kDa were not able to reduce Au (III) to Au (0). Interestingly, when comparing the AuNPs formation ability of various fungal extractions, it was found that while extractions containing large biomolecules were not capable of forming NPs, others containing small components would make unstable NPs, likely due to the small components' inability to act as stabilizing

agents. Combining different fractions developed stable NPs with slightly increased sizes of ~30 nm, compared to previous sizes of ~8–30 nm. Thus, it was concluded that biomolecules <3 kDa, such as glucose or amino acids, are involved in reducing the metal, and biomolecules >3 kDa, such as proteins, are involved in the stabilization [54].

2. Antifungal Classes and Combination with Nanoparticles

Currently, there are six antifungal drug categories, including four main antifungal drug classes: allylamines, azoles, echinocandins, and polyenes. Some literature will include the antimetabolite class [61][62] and, more recently, triterpenoids, such as ibrexafungerp, the first drug in the triterpenoid class [61][63].

Ergosterol and β-(1,3)-D-glucan are favored targets in antifungals, as these molecules are crucial for the survival of pathogenic fungi. These compounds are attractive because they are not produced by human cells (**Table 7**) [61]. Ergosterol is essentially the cholesterol equivalent in fungi and protozoa. Found in the cellular membrane, it is responsible for the membrane's integrity and flexibility. Ergosterol is structurally similar to cholesterol aside from containing a double bond and additional methyl group in the alkyl side chain; this trans double bond means it is not saturated like cholesterol. There is also a second double bond at 7,8-position, alongside the 5,6-positioned double bond found in the cholesterol [64].

Table 7. Current antifungal classes and their mechanisms of action.

Class	Examples	Mechanism of Action
Allylamines	Terbinafine Naftifine	Squalene epoxidase inhibition, responsible for conversion of squalene to ergosterol
Azoles	Clotrimazole Miconazole Ketoconazole Fluconazole Itrazonacole	C14-α demethylation inhibition of lanosterol, inhibiting ergosterol synthesis
Echinocandins	Caspofungin Micafungin Anidulafungin	β-(1,3)-D-glucan synthase inhibition, interfering with cell wall synthesis
Polyenes	Amphotericin B Nystatin Candicidin	Ergosterol binding, forming pores and causing leakage, inhibiting proper transport mechanisms
Antimetabolites	Flucytosine	Pyrimidine analogue, interfering with nucleic acid synthesis
Triterpenoids	Ibrexafungerp	β-(1,3)-D-glucan synthase inhibition, interfering with cell wall synthesis

As mentioned earlier, the second compound, β-(1,3)-D-glucan, is a fungal cell wall component.

Antifungal resistance is a problem that is increasing worldwide. This can arise due to many mechanisms, including gene upregulation [65] for cell wall component synthesis [66] or efflux pump synthesis [67], modification of target site

[68], or development of biofilm [69], amongst others. For example, the overexpression of *ERG11* in yeast or *CYP51* in mold confers resistance through the overproduction of lanosterol 14-α demethylase, aiding cell wall building and maintenance [66][70]. Because NPs have numerous mechanisms of action, fungi would have to evolve in multiple ways to acquire resistance while maintaining homeostasis and survival. As it is difficult to combat the simultaneous antifungal mechanisms of NPs, even though some are similar to antifungals (e.g., gene regulation), it is unlikely that fungi would be able to become resistant, at the very least, not at the same rate as the current antifungals used today.

NPs can be synthesized and combined with antifungals to increase one or both of their antimycotic capabilities [8][20][28][56][57][71]. One study decorated SiNPs with amphotericin B (AmB) to create particles with antifungal ability that could adhere to surfaces and be reused up to 5 times. The NPs alone was 3–33 times less effective than AmB on their own, but the addition of the antifungal gave the NPs an antifungal ability stronger than that of 10 nm colloidal Ag [20]. This, paired with the ability to coat surfaces, makes the particles worth further investigation, particularly in coating medical devices. While many studies have shown the synergism of NPs combined with antifungal medications, the effect can vary based on which fungal species are being treated [56][57].

The addition of antifungals to NPs can also benefit efficacy in unexpected ways. It can increase the roughness of NPs surfaces, which may account for mechanical damage or increased surface areas [28]. When antifungals are enclosed in NPs rather than coated, this can reduce their toxicity, such as in the case of AmB, where hemolytic activity in mammalian red blood cells was reduced from approximately 66% to 30% [72]. Therefore, combining NPs with antifungals can enhance activity, alter the morphology of NPs, and reduce cytotoxicity in human cells. Also, NPs on their own can have stronger antimycotic abilities than traditional antifungals [12].

References

1. Lee, Y.; Puumala, E.; Robbins, N.; Cowen, L.E. Antifungal drug resistance: Molecular mechanisms in Candida albicans and beyond. Chem. Rev. 2021, 121, 3390–3411.
2. Kim, K.J.; Sung, W.S.; Suh, B.K.; Moon, S.K.; Choi, J.S.; Kim, J.G.; Lee, D.G. Antifungal activity and mode of action of silver nano-particles on Candida albicans. Biometals 2009, 22, 235–242.
3. Wang, D.; Xue, B.; Wang, L.; Zhang, Y.; Liu, L.; Zhou, Y. Fungus-mediated green synthesis of nano-silver using Aspergillus sydowii and its antifungal/antiproliferative activities. Sci. Rep. 2021, 11, 10356.
4. Monteiro, D.R.; Gorup, L.F.; Silva, S.; Negri, M.; De Camargo, E.R.; Oliveira, R.; Barbosa, D.D.B.; Henriques, M. Silver colloidal nanoparticles: Antifungal effect against adhered cells and biofilms of Candida albicans and Candida glabrata. Biofouling 2011, 27, 711–719.
5. Auyeung, A.; Casillas-Santana, M.A.; Martinez-Castanon, G.A.; Slavin, Y.N.; Zhao, W.; Asnis, J.; Häfeli, U.O.; Bach, H. Effective control of molds using a combination of nanoparticles. PLoS ONE

2017, 12, e0169940.

6. Panáček, A.; Kolář, M.; Večeřová, R.; Prucek, R.; Soukupová, J.; Kryštof, V.; Hamal, P.; Zbořil, R.; Kvítek, L. Antifungal activity of silver nanoparticles against Candida spp. Biomaterials 2009, 30, 6333–6340.
7. Xia, Z.K.; Ma, Q.H.; Li, S.Y.; Zhang, D.Q.; Cong, L.; Tian, Y.L.; Yang, R.Y. The antifungal effect of silver nanoparticles on Trichosporon asahii. J. Microbiol. Immunol. Infect. 2016, 49, 182–188.
8. Różalska, B.; Sadowska, B.; Budzyńska, A.; Bernat, P.; Różalska, S. Biogenic nanosilver synthesized in Metarhizium robertsii waste mycelium extract—As a modulator of Candida albicans morphogenesis, membrane lipidome and biofilm. PLoS ONE 2018, 13, e0194254.
9. Pereira, L.; Dias, N.; Carvalho, J.; Fernandes, S.; Santos, C.; Lima, N. Synthesis, characterization and antifungal activity of chemically and fungal-produced silver nanoparticles against Trichophyton rubrum. J. Appl. Microbiol. 2014, 117, 1601–1613.
10. Chen, J.; Sun, L.; Cheng, Y.; Lu, Z.; Shao, K.; Li, T.; Hu, C.; Han, H. Graphene oxide-silver nanocomposite: Novel agricultural antifungal agent against Fusarium graminearum for crop disease prevention. ACS Appl. Mater. Interfaces 2016, 8, 24057–24070.
11. Martinez-Gutierrez, F.; Olive, P.L.; Banuelos, A.; Orrantia, E.; Nino, N.; Sanchez, E.M.; Ruiz, F.; Bach, H.; Av-Gay, Y. Synthesis, characterization, and evaluation of antimicrobial and cytotoxic effect of silver and titanium nanoparticles. Nanomedicine 2010, 6, 681–688.
12. Selvaraj, M.; Pandurangan, P.; Ramasami, N.; Rajendran, S.B.; Sangilimuthu, S.N.; Perumal, P. Highly potential antifungal activity of quantum-sized silver nanoparticles against Candida albicans. Appl. Biochem. Biotechnol. 2014, 173, 55–66.
13. Martínez, A.; Apip, C.; Meléndrez, M.F.; Domínguez, M.; Sánchez-Sanhueza, G.; Marzialetti, T.; Catalán, A. Dual antifungal activity against Candida albicans of copper metallic nanostructures and hierarchical copper oxide marigold-like nanostructures grown in situ in the culture medium. J. Appl. Microbiol. 2021, 130, 1883–1892.
14. Prucek, R.; Tuček, J.; Kilianová, M.; Panáček, A.; Kvítek, L.; Filip, J.; Kolář, M.; Tománková, K.; Zbořil, R. The targeted antibacterial and antifungal properties of magnetic nanocomposite of iron oxide and silver nanoparticles. Biomaterials 2011, 32, 4704–4713.
15. Zamperini, C.A.; André, R.S.; Longo, V.M.; Mima, E.G.; Vergani, C.E.; Machado, A.L.; Varela, J.A.; Longo, E. Antifungal applications of Ag-decorated hydroxyapatite nanoparticles. J. Nanomater. 2013, 2013, e174398.
16. De la Rosa-García, S.C.; Martínez-Torres, P.; Gómez-Cornelio, S.; Corral-Aguado, M.A.; Quintana, P.; Gómez-Ortíz, N.M. Antifungal activity of ZnO and MgO nanomaterials and their mixtures against Colletotrichum gloeosporioides strains from tropical fruit. J. Nanomater. 2018, 2018, e3498527.

17. Athie-García, M.S.; Piñón-Castillo, H.A.; Muñoz-Castellanos, L.N.; Ulloa-Ogaz, A.L.; Martínez-Varela, P.I.; Quintero-Ramos, A.; Duran, R.; Murillo-Ramirez, J.G.; Orrantia-Borunda, E. Cell wall damage and oxidative stress in Candida albicans ATCC 10231 and Aspergillus niger caused by palladium nanoparticles. Toxicol. Vitr. 2018, 48, 111–120.
18. Parsameher, N.; Rezaei, S.; Khodavasiy, S.; Salari, S.; Hadizade, S.; Kord, M.; Mousavi, S.A.A. Effect of biogenic selenium nanoparticles on ERG11 and CDR1 gene expression in both fluconazole-resistant and -susceptible Candida albicans isolates. Curr. Med. Mycol. 2017, 3, 16–20.
19. Bafghi, M.H.; Nazari, R.; Darroudi, M.; Zargar, M.; Zarrinfar, H. The effect of biosynthesized selenium nanoparticles on the expression of CYP51A and HSP90 antifungal resistance genes in Aspergillus fumigatus and Aspergillus flavus. Biotechnol. Prog. 2022, 38, e3206.
20. Paulo, C.S.O.; Vidal, M.; Ferreira, L.S. Antifungal nanoparticles and surfaces. Biomacromolecules 2010, 11, 2810–2817.
21. Hosseini, S.S.; Ghaemi, E.; Noroozi, A.; Niknejad, F. Zinc oxide nanoparticles inhibition of initial adhesion and ALS1 and ALS3 gene expression in Candida albicans strains from urinary tract infections. Mycopathologia 2019, 184, 261–271.
22. Hosseini, S.S.; Joshaghani, H.; Shokohi, T.; Ahmadi, A.; Mehrbakhsh, Z. Antifungal activity of ZnO nanoparticles and nystatin and downregulation of SAP1-3 genes expression in fluconazole-resistant Candida albicans isolates from vulvovaginal candidiasis. Infect. Drug Resist. 2020, 13, 385–394.
23. Jebali, A.; Hajjar, F.H.E.; Pourdanesh, F.; Hekmatimoghaddam, S.; Kazemi, B.; Masoudi, A.; Daliri, K.; Sedighi, N. Silver and gold nanostructures: Antifungal property of different shapes of these nanostructures on Candida species. Med. Mycol. 2014, 52, 65–72.
24. Ahmad, T.; Wani, I.A.; Lone, I.H.; Ganguly, A.; Manzoor, N.; Ahmad, A.; Ahmed, J.; Al-Shihri, A.S. Antifungal activity of gold nanoparticles prepared by solvothermal method. Mater. Res. Bull. 2013, 48, 12–20.
25. Ing, L.Y.; Zin, N.M.; Sarwar, A.; Katas, H. Antifungal activity of chitosan nanoparticles and correlation with their physical properties. Int. J. Biomat. 2012, 2012, 632698.
26. Bramhanwade, K.; Shende, S.; Bonde, S.; Gade, A.; Rai, M. Fungicidal activity of Cu nanoparticles against Fusarium causing crop diseases. Environ. Chem. Lett. 2016, 14, 229–235.
27. Osonga, F.J.; Kalra, S.; Miller, R.M.; Isika, D.; Sadik, O.A. Synthesis, characterization and antifungal activities of eco-friendly palladium nanoparticles. RSC Adv. 2020, 10, 5894–5904.
28. Abid, S.; Uzair, B.; Niazi, M.B.K.; Fasim, F.; Bano, S.A.; Jamil, N.; Batool, R.; Sajjad, S. Bursting the virulence traits of MDR strain of Candida albicans using sodium alginate-based microspheres containing nystatin-loaded MgO/CuO nanocomposites. Int. J. Nanomed. 2021, 16, 1157–1174.

29. Chougale, R.; Kasai, D.; Nayak, S.; Masti, S.; Nasalapure, A.; Raghu, A.V. Design of eco-friendly PVA/TiO2 based nanocomposites and their antifungal activity study. Green Mater. 2020, 8, 40–48.
30. Pulit, J.; Banach, M.; Szczygłowska, R.; Bryk, M. Nanosilver against fungi. Silver nanoparticles as an effective biocidal factor. Acta Biochim. Pol. 2013, 60, 795–798.
31. Guerra, J.D.; Sandoval, G.; Avalos-Borja, M.; Pestryakov, A.; Garibo, D.; Susarrey-Arce, A.; Bogdanchikova, N. Selective antifungal activity of silver nanoparticles: A comparative study between Candida tropicalis and Saccharomyces boulardii. Colloids Interface Sci. Commun. 2020, 37, 100280.
32. Aguilar-Méndez, M.A.; San Martín-Martínez, E.; Ortega-Arroyo, L.; Cobián-Portillo, G.; Sánchez-Espíndola, E. Synthesis and characterization of silver nanoparticles: Effect on phytopathogen Colletotrichum gloesporioides. J. Nanopart. Res. 2011, 13, 2525–2532.
33. Arciniegas-Grijalba, P.A.; Patiño-Portela, M.C.; Mosquera-Sánchez, L.P.; Guerrero-Vargas, J.A.; Rodríguez-Páez, J.E. ZnO nanoparticles (ZnO-NPs) and their antifungal activity against coffee fungus Erythricium salmonicolor. Appl. Nanosci. 2017, 7, 225–241.
34. Kim, S.W.; Jung, J.H.; Lamsal, K.; Kim, Y.S.; Min, J.S.; Lee, Y.S. Antifungal effects of silver nanoparticles (AgNPs) against various plant pathogenic fungi. Mycobiology 2012, 40, 53–58.
35. Mishra, S.; Singh, B.R.; Singh, A.; Keswani, C.; Naqvi, A.H.; Singh, H.B. Biofabricated silver nanoparticles act as a strong fungicide against Bipolaris sorokiniana causing spot blotch disease in wheat. PLoS ONE 2014, 9, e97881.
36. Zhao, J.; Wang, L.; Xu, D.; Lu, Z. Involvement of ROS in nanosilver-caused suppression of aflatoxin production from Aspergillus flavus. RSC Adv. 2017, 7, 23021–23026.
37. Tiwari, A.K.; Gupta, M.K.; Pandey, G.; Tilak, R.; Narayan, R.J.; Pandey, P.C. Size and zeta potential clicked germination attenuation and anti-sporangiospores activity of PEI-functionalized silver nanoparticles against COVID-19 associated Mucorales (Rhizopus arrhizus). Nanomaterials 2022, 12, 2235.
38. Abdelrhim, A.; Mazrou, Y.; Nehela, Y.; Atallah, O.; El-Ashmony, R.; Dawood, M. Silicon dioxide nanoparticles induce innate immune responses and activate antioxidant machinery in wheat against Rhizoctonia solani. Plants 2021, 10, 2758.
39. Cioffi, N.; Torsi, L.; Ditaranto, N.; Tantillo, G.; Ghibelli, L.; Sabbatini, L.; Bleve-Zacheo, T.; D'Alessio, M.; Zambonin, P.G.; Traversa, E. Copper nanoparticle/polymer composites with antifungal and bacteriostatic properties. Chem. Mater. 2005, 17, 5255–5262.
40. Alexander, J.W. History of the medical use of silver. Surg. Infect. 2009, 10, 289–292.
41. Xiong, Y.; Brunson, M.; Huh, J.; Huang, A.; Coster, A.; Wendt, K.; Fay, J.; Qin, D. The role of surface chemistry on the toxicity of Ag nanoparticles. Small 2013, 9, 2628–2638.

42. Kim, S.W.; Kim, K.S.; Lamsal, K.; Kim, Y.J.; Kim, S.B.; Jung, M.Y.; Sim, S.J.; Kim, H.S.; Chang, S.J.; Kim, J.K.; et al. An in vitro study of the antifungal effect of silver nanoparticles on oak wilt pathogen Raffaelea sp. J. Microb. Microbiol. 2009, 19, 760–764.
43. Ouda, S.M. Antifungal activity of silver and copper nanoparticles on two plant pathogens, Alternaria alternata and Botrytis cinerea. Res. J. Microbiol. 2014, 9, 34–42.
44. Sousa, C.A.; Soares, H.M.V.M.; Soares, E.V. Metal(loid) oxide (Al2O3, Mn3O4, SiO2 and SnO2) nanoparticles cause cytotoxicity in yeast via intracellular generation of reactive oxygen species. Appl. Microbiol. Biotechnol. 2019, 103, 6257–6269.
45. Eda, G.; Fanchini, G.; Chhowalla, M. Large-area ultrathin films of reduced graphene oxide as a transparent and flexible electronic material. Nat. Nanotech. 2008, 3, 270–274.
46. Mukherjee, K.; Acharya, K.; Biswas, A.; Jana, N.R. TiO2 nanoparticles co-doped with nitrogen and fluorine as visible-light-activated antifungal agents. ACS Appl. Nano Mater. 2020, 3, 2016–2025.
47. Boxi, S.S.; Mukherjee, K.; Paria, S. Ag doped hollow TiO2 nanoparticles as an effective green fungicide against Fusarium solani and Venturia inaequalis phytopathogens. Nanotechnology 2016, 27, 085103.
48. Wani, A.H.; Shah, M.A. A unique and profound effect of MgO and ZnO nanoparticles on some plant pathogenic fungi. J. Appl. Pharm. Sci. 2012, 2, 40–44.
49. He, L.; Liu, Y.; Mustapha, A.; Lin, M. Antifungal activity of zinc oxide nanoparticles against Botrytis cinerea and Penicillium expansum. Microbiol. Res. 2011, 166, 207–215.
50. Navale, G.R.; Shinde, S.S. Antimicrobial activity of ZnO nanoparticles against pathogenic bacteria and fungi. JSM Nanotechnol. Nanomed. 2015, 3, 1033.
51. Babele, P.K.; Thakre, P.K.; Kumawat, R.; Tomar, R.S. Zinc oxide nanoparticles induce toxicity by affecting cell wall integrity pathway, mitochondrial function and lipid homeostasis in Saccharomyces cerevisiae. Chemosphere 2018, 213, 65–75.
52. Kumari, M.; Giri, V.P.; Pandey, S.; Kumar, M.; Katiyar, R.; Nautiyal, C.S.; Mishra, A. An insight into the mechanism of antifungal activity of biogenic nanoparticles than their chemical counterparts. Pestic. Biochem. Physiol. 2019, 157, 45–52.
53. Kalagatur, N.K.; Nirmal Ghosh, O.S.; Sundararaj, N.; Mudili, V. Antifungal activity of chitosan nanoparticles encapsulated with Cymbopogon martinii essential oil on plant pathogenic fungi Fusarium graminearum. Front. Pharmacol. 2018, 9, 610.
54. Molnár, Z.; Bódai, V.; Szakacs, G.; Erdélyi, B.; Fogarassy, Z.; Sáfrán, G.; Varga, T.; Kónya, Z.; Tóth-Szeles, E.; Szűcs, R.; et al. Green synthesis of gold nanoparticles by thermophilic filamentous fungi. Sci. Rep. 2018, 8, 3943.

55. Ruiz-Romero, P.; Valdez-Salas, B.; González-Mendoza, D.; Mendez-Trujillo, V. Antifungal effects of silver phytonanoparticles from Yucca shilerifera against strawberry soil-borne pathogens: Fusarium solani and Macrophomina phaseolina. Mycobiology 2018, 46, 47–51.

56. Gajbhiye, M.; Kesharwani, J.; Ingle, A.; Gade, A.; Rai, M. Fungus-mediated synthesis of silver nanoparticles and their activity against pathogenic fungi in combination with fluconazole. Nanomedicine 2009, 5, 382–386.

57. Singh, M.; Kumar, M.; Kalaivani, R.; Manikandan, S.; Kumaraguru, A.K. Metallic silver nanoparticle: A therapeutic agent in combination with antifungal drug against human fungal pathogen. Bioprocess. Biosyst. Eng. 2013, 36, 407–415.

58. Li, X.; Xu, H.; Chen, Z.-S.; Chen, G. Biosynthesis of nanoparticles by microorganisms and their applications. J. Nanomater. 2011, 2011, 1–16.

59. He, S.; Guo, Z.; Zhang, Y.; Zhang, S.; Wang, J.; Gu, N. Biosynthesis of gold nanoparticles using the bacteria Rhodopseudomonas capsulata. Mater. Lett. 2007, 61, 3984–3987.

60. Durán, N.; Marcato, P.D.; Alves, O.L.; De Souza, G.I.; Esposito, E. Mechanistic aspects of biosynthesis of silver nanoparticles by several Fusarium oxysporum strains. J. Nanobiotechnol. 2005, 3, 8.

61. Gintjee, T.J.; Donnelley, M.A.; Thompson, G.R. Aspiring antifungals: Review of current antifungal pipeline developments. J. Fungi. 2020, 6, 28.

62. Dixon, D.M.; Walsh, T.J. Chapter 76 Antifungal agents. In Medical Microbiology, 4th ed.; University of Texas Medical Branch at Galveston: Galveston, TX, USA, 1996.

63. Jallow, S.; Govender, N.P. Ibrexafungerp: A first-in-class oral triterpenoid glucan synthase inhibitor. J. Fungi. 2021, 7, 163.

64. Cournia, Z.; Ullmann, G.M.; Smith, J.C. Differential effects of cholesterol, ergosterol and lanosterol on a dipalmitoyl phosphatidylcholine membrane: A molecular dynamics simulation study. J. Phys, Chem. B 2007, 111, 1786–1801.

65. Vermitsky, J.-P.; Earhart, K.D.; Smith, W.L.; Homayouni, R.; Edlind, T.D.; Rogers, P.D. Pdr1 regulates multidrug resistance in Candida glabrata: Gene disruption and genome-wide expression studies. Mol. Microbiol. 2006, 61, 704–722.

66. Flowers, S.A.; Barker, K.S.; Berkow, E.L.; Toner, G.; Chadwick, S.G.; Gygax, S.E.; Morschhäuser, J.; Rogers, P.D. Gain-of-function mutations in UPC2 are a frequent cause of ERG11 upregulation in azole-resistant clinical isolates of Candida albicans. Eukaryot. Cell 2012, 11, 1289–1299.

67. Morschhäuser, J.; Barker, K.S.; Liu, T.T.; Blaß-Warmuth, J.; Homayouni, R.; Rogers, P.D. The transcription factor Mrr1p controls expression of the MDR1 efflux pump and mediates multidrug resistance in Candida albicans. PLoS Pathog. 2007, 3, e164.

68. Sagatova, A.A.; Keniya, M.V.; Wilson, R.K.; Monk, B.C.; Tyndall, J.D.A. Structural insights into binding of the antifungal drug fluconazole to Saccharomyces cerevisiae lanosterol 14α-demethylase. Antimicrob. Agents Chemother. 2015, 59, 4982–4989.
69. Chandra, J.; Kuhn, D.M.; Mukherjee, P.K.; Hoyer, L.L.; McCormick, T.; Ghannoum, M.A. Biofilm formation by the fungal pathogen Candida albicans: Development, architecture, and drug resistance. J. Bacteriol. 2001, 183, 5385–5394.
70. Marichal, P.; Koymans, L.; Willemsens, S.; Bellens, D.; Verhasselt, P.; Luyten, W.; Borgers, M.; Ramaekers, F.C.; Odds, F.C.; Bossche, H.V. Contribution of mutations in the cytochrome P450 14α-demethylase (Erg11p, Cyp51p) to azole resistance in Candida albicans. Microbiology 1999, 145, 2701–2713.
71. Liu, Y.; Cui, X.; Zhao, L.; Zhang, W.; Zhu, S.; Ma, J. Chitosan nanoparticles to enhance the inhibitory effect of natamycin on Candida albicans. J. Nanomater. 2021, 2021, 6644567.
72. Yang, M.; Du, K.; Hou, Y.; Xie, S.; Dong, Y.; Li, D.; Du, Y. Synergistic antifungal effect of amphotericin B-loaded poly(lactic-co-glycolic acid) nanoparticles and ultrasound against Candida albicans biofilms. Antimicrob. Agents Chemother. 2019, 63, e02022-18.